

# Linking metal centres with 1,4-bis(diphenylphosphino)but-2-yne (DPPBu): syntheses and molecular structures of $[\{\text{Mo}(\text{CO})_4(\mu\text{-DPPBu})\}_2]$ and $[\{\text{Mo}(\text{CO})_4(\eta^2\text{-DPPBu})\}_3\{\text{Mo}(\text{CO})\}]$

Graeme Hogarth<sup>\*</sup>, Jim Yau Pang

Chemistry Department, University College London, 20 Gordon Street, London, WC1H 0AJ, UK

Received 19 October 1995

## Abstract

Addition of *cis*- $[\text{Mo}(\text{CO})_4(\text{piperidine})]$  to 1,4-bis(diphenylphosphino)but-2-yne (DPPBu) affords  $[\{\text{Mo}(\text{CO})_4(\mu\text{-DPPBu})\}_2]$  (**1**) and  $[\{\text{Mo}(\text{CO})_4(\eta^2\text{-DPPBu})\}_3\{\text{Mo}(\text{CO})\}]$  (**2**), both of which have been characterised crystallographically. Three different bonding modes of the diphosphine are seen in the two complexes. In **1** it bridges molybdenum tetracarbonyl centres via coordination through phosphorus to give a 14-membered ring with a chair-like configuration, while in **2** the diphosphine chelates molybdenum tetracarbonyl centres, and three of these units are further complexed to a molybdenum carbonyl fragment via coordination of the carbon–carbon triple bonds.

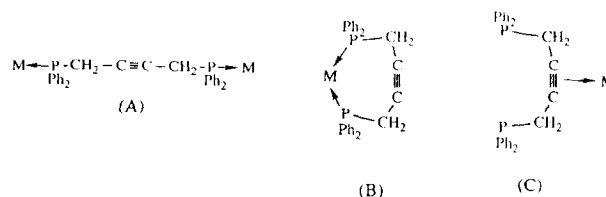
**Keywords:** Diphosphine; Molybdenum; Alkyne; Crystal structure; Chelation; Fluxionality; Bridging ligand

## 1. Introduction

We have recently been concerned with the synthesis of binuclear complexes in which two Group 6 tetracarbonyl centres are linked together by rigid-backbone bidentate [1,2] or tetradentate [3] phosphine ligands. For example, we have prepared and crystallographically characterised  $[\{\text{Mo}(\text{CO})_4(\mu\text{-DPPA})\}_2]$  [**1**], in which the centres are spanned by two molecules of bis(diphenylphosphino)acetylene (DPPA) to afford a 10-membered dimetallacyclic ring. In this complex, the two carbon–carbon triple bonds of diphosphine backbones are held in relatively close proximity as a result of a pronounced twisting of the ring, the closest contact being 3.4 Å, with the two bonds twisted by some 38.3° with respect to one another. We considered that if the two triple bonds could be brought into closer contact, it may be possible to photochemically or thermally induce carbon–carbon bond formation to afford convenient preparation of a tetrahedrane [4] by what, in effect, would be a template reaction. Clearly, in order to have any chance of doing this, a greater degree of conformational flexibility would need to be built into the molecule. The

simplest way of doing this is to introduce flexible methylene units into the backbone of the diphosphine, that is to use 1,4-bis(diphenylphosphino)but-2-yne (DPPBu) to link together the metal centres. The synthesis of DPPBu has previously been described by two groups [5,6], however, surprisingly in view of the preponderance of DPPA chemistry [7], and as far as we can ascertain, the chemistry of the more flexible DPPBu ligand has been the subject of only one publication [6]. Thus, as long ago as 1970, King and Efraty [6] described the synthesis of a number of complexes in which DPPBu spanned two metal centres. Most relevant to our work, they prepared two complexes  $[\{\text{Ni}(\text{CO})_2(\mu\text{-DPPBu})\}_2]$  and  $[\{\text{PtCl}_2(\mu\text{-DPPBu})\}_2]$  in which two diphosphines were proposed to span metal centres.

The DPPBu ligand can potentially bind to metal centres in a number of different ways, some of which (A–C) are shown below:



<sup>\*</sup> Corresponding author.

Mode A is that previously observed by King and Efraty which closely mimics the coordination chemistry of DPPA. Unlike the less flexible DPPA ligand, however, coordination to a single metal centre through both phosphorus centres (B) may be possible, while it can also potentially bind as a simple alkyne (C) in a manner analogous to that seen occasionally in DPPA chemistry [8]. Herein we report details of the reaction of DPPBu with *cis*-[Mo(CO)<sub>4</sub>(piperidine)<sub>2</sub>], which results in the formation of two crystallographically characterised products within which all three bonding modes (A–C) of DPPBu are observed.

## 2. Experimental details

### 2.1. General comments

All reactions were carried out under N<sub>2</sub> in predried solvents. NMR spectra were recorded on a Varian VXR 400 spectrometer and IR spectra on a Nicolet 205 Fourier transform spectrometer. Chromatography was carried out on columns of deactivated alumina (6% w/w water). Elemental analyses were performed in the Chemistry Department of University College London. 1,4-Bis(diphenylphosphino)but-2-yne (DPPBu) [6] and *cis*-[Mo(CO)<sub>4</sub>(piperidine)<sub>2</sub>] [9] were prepared by literature methods.

### 2.2. Synthesis of $\{[Mo(CO)_4(\mu-DPPBu)]_2\}$ (1) and $\{[Mo(CO)_4(\eta^2-DPPBu)]_3\{Mo(CO)\}_3\}$ (2)

A THF solution (100 cm<sup>3</sup>) of *cis*-[Mo(CO)<sub>4</sub>(piperidine)<sub>2</sub>] (2.80 g, 7.36 mmol) and DPPBu (7.39 mmol) were stirred at room temperature for 16 h, resulting in the formation of a red–brown solution. Removal of volatiles at reduced pressure afforded a red–brown solid which was washed with light petroleum (2 × 50 cm<sup>3</sup>). Analysis of the crude material by <sup>31</sup>P NMR spectroscopy revealed the presence of 1–3 in an approximate 10:5:1 ratio respectively. Chromatography of about half of the yellow solid resulted in the elution with light petroleum/dichloromethane (7:3) of a yellow band which afforded approximately 1 g of a yellow powder. A <sup>31</sup>P NMR spectrum of the band revealed that the relative amount of 3 had diminished substantially. The material was split up into portions and fractional recrystallisation attempted from a number of solvent mixtures. Slow diffusion of methanol into a dichloromethane solution led to the deposition of well-formed colourless crystals of 1 while in contrast, from a 1,2-dichloropropane–light petroleum mixture, yellow plates of 2 were deposited. Owing to the nature of the separation and purification procedure, yields of 1 and 2 are difficult to estimate, but up to 100 mg of pure complexes were isolated. We were unable to isolate a pure

sample of 3. Standing a chloroform solution of the mixture (before chromatography) in air led to a gradual clouding of the solution over 10 days. After filtration, <sup>31</sup>P NMR spectroscopy showed the complete absence of 1, while 2 and 3 were present in an approximate 4:1 ratio.

$\{[Mo(CO)_4(\mu-DPPBu)]_2\}$  (1). Anal. Found: C, 57.31; H, 3.66. Mo<sub>2</sub>C<sub>64</sub>H<sub>48</sub>O<sub>8</sub>P<sub>4</sub> · CH<sub>2</sub>Cl<sub>2</sub>. Calc.: C, 57.99; H, 3.72%. <sup>1</sup>H NMR (CDCl<sub>3</sub>) (293 K) δ 7.35–7.26 (m, 40H, Ph), 2.92 (s, 8H, CH<sub>2</sub>). <sup>31</sup>P NMR (CDCl<sub>3</sub>) δ 27.0 (s). IR (CH<sub>2</sub>Cl<sub>2</sub>) 2022(m), 1918(sh), 1906(s) cm<sup>-1</sup>.

$\{[Mo(CO)_4(\eta^2-DPPBu)]_3\{Mo(CO)\}_3\}$  (2). Anal. Found: C, 55.60; H, 3.79. Mo<sub>4</sub>C<sub>99</sub>H<sub>72</sub>O<sub>13</sub>P<sub>6</sub> · 4H<sub>2</sub>O. Calc.: C, 56.30; H, 3.79%. <sup>1</sup>H NMR (CDCl<sub>3</sub>) δ 7.36–7.15 (m, 60H, Ph), 4.35 (m, 4H, CH<sub>2</sub>), 3.24 (m, 4H, CH<sub>2</sub>). <sup>31</sup>P NMR (CDCl<sub>3</sub>) δ 30.6 (d, J 27.7 Hz), 26.3 (d, J 27.7 Hz), IR (CH<sub>2</sub>Cl<sub>2</sub>) 2066(w), 2022(s), 1922(sh), 1899 (s) cm<sup>-1</sup>.

3. <sup>31</sup>P NMR (CDCl<sub>3</sub>) δ 28.8 (d, J 23.5 Hz), 23.5 (d, J 23.5 Hz).

### 2.3. X-ray data collection and solution

A colourless single crystal of 1 · MeOH of approximate size 0.42 × 0.30 × 0.16 mm<sup>3</sup> was mounted on a glass fibre. All geometric and intensity data were taken from this sample using an automated four-circle diffractometer (Nicolet R3mV) equipped with Mo Kα radiation (λ = 0.71073 Å). The lattice vectors were identified by application of the automatic indexing routine of the diffractometer to the positions of 28 reflections taken from a rotation photograph and centred by the diffractometer. The ω–2θ technique was used to measure 5985 reflections (5688 unique) in the range 5° ≤ 2θ ≤ 50°. Three standard reflections (remeasured every 97 scans) showed no significant loss in intensity during data collection. The data were corrected for Lorentz and polarisation effects, and empirically for absorption. The 4573 unique data with I ≥ 3.0σ(I) were used to solve and refine the structure in the monoclinic space group P $\bar{1}$ .

The structure was solved by Patterson methods and developed by using alternating cycles of least-squares refinement and difference-Fourier synthesis. The non-hydrogen atoms were refined anisotropically, except those of the methanol which were refined isotropically. Hydrogens were placed in idealised positions (C–H 0.96 Å) and assigned a common isotropic thermal parameter (U = 0.08 Å<sup>2</sup>). The carbon of the methanol was disordered over two sites (70:30). The final cycle of least-squares refinement included 364 parameters for 4321 variables and did not shift any parameter by more than 0.03 times its standard deviation. The final R values were 0.060 and 0.060. The final difference-Fourier contained three peaks greater than 1.00 e Å<sup>-3</sup>, all lying close to the methanol. Structure solution used the

SHELXTL PLUS program package on a microVax II computer [10].

Crystallographic analysis of  $2 \cdot 4H_2$  was carried out in an analogous manner on a yellow single crystal of approximate size  $0.60 \times 0.44 \times 0.08 \text{ mm}^3$ . Owing to the large cell volume, reflections were only measured in the range  $5^\circ \leq 2\theta \leq 42^\circ$  and the data were not corrected empirically for absorption. Non-hydrogen atoms were refined anisotropically, except the phenyl rings and water of crystallisation which were refined isotropically. All important crystallographic parameters for both complexes are summarised in Table 1 and atomic coordinates and equivalent isotropic displacement parameters are given in Tables 2 and 3 for **1** and **2** respectively. Complete lists of bond lengths and angles and tables of hydrogen atom coordinates and anisotropic thermal parameters have been deposited with the Cambridge Crystallographic Data Centre.

### 3. Results and discussion

Addition of DPPBu to a THF solution of *cis*- $[Mo(CO)_4(\text{piperidine})_2]$  at room temperature resulted in a slow reaction, as monitored by IR spectroscopy, to afford three new species **1–3** in an approximate 10:5:1 ratio respectively as shown by  $^{31}P$  NMR spectroscopy.

The three could not be separated by column chromatography, which did serve to remove organic impurities while significantly reducing the relative amount of **3**. Analytically pure samples of the two major products,  $[Mo(CO)_4(\mu\text{-DPPBu})_2]$  (**1**) and  $[Mo(CO)_4(\eta^2\text{-DPPBu})_3\{Mo(CO)\}]$  (**2**), were obtained upon fractional crystallisation. Thus, colourless crystals of **1** formed upon slow diffusion of methanol into a dichloromethane solution, while yellow **2** was obtained from a 1,2-dichloropropane–light petroleum solution. While isolated yields were low (ca. 5–10%), a combined yield of the crude product after chromatography was about 60%. Characterisation of both **1** and **2** was made on the basis of analytical, spectroscopic and X-ray crystallographic analysis.

The anticipated reaction product, namely dimetallacyclic  $[Mo(CO)_4(\mu\text{-DPPBu})_2]$  (**1**), was easily identified on the basis of spectroscopic and analytical data. The IR spectrum was characteristic of a *cis*-disubstituted molybdenum tetracarbonyl fragment, while the observation of a singlet at  $\delta$  27.0 in the  $^{31}P$  NMR spectrum was indicative of equivalent, metal-coordinated, phosphorus centres. At room temperature the  $^1H$  NMR spectrum was deceptively simple, consisting of a narrow multiplet in the aromatic region and a lower field singlet at  $\delta$  2.92 assigned to equivalent methylene protons. The latter appears at first sight to be inconsis-

Table 1  
Crystallographic data for **1** · MeOH and **2** ·  $4H_2O$

	<b>1</b> · MeOH	<b>2</b> · $4H_2O$
Formula	$Mo_2C_{65}H_{52}O_9P_4$	$Mo_4C_{97}H_{80}O_{17}P_6$
Space group	$P\bar{1}$	$P2_1/a$
Colour	Colourless	Yellow
$a(\text{\AA})$	11.0013(36)	20.2021(58)
$b(\text{\AA})$	11.8462(27)	22.2561(34)
$c(\text{\AA})$	14.0292(41)	22.7436(69)
$\alpha(\text{deg})$	87.011(21)	90.0
$\beta(\text{deg})$	71.855(24)	90.398(24)
$\gamma(\text{deg})$	63.258(19)	90.0
$V(\text{\AA}^3)$	15433.22	10225.75
Z	1	4
$F(000)$	658	4224
$d_{\text{calc}}(\text{g cm}^{-3})$	1.39	1.36
Crystal size ( $\text{mm}^3$ )	$0.42 \times 0.30 \times 0.16$	$0.60 \times 0.44 \times 0.08$
$\mu(\text{Mo K}\alpha)(\text{cm}^{-1})$	5.50	6.17
Orient. reflections: no.; range	28; $17 \leq 2\theta \leq 28$	24; $14 \leq 2\theta \leq 24$
Data measured	5985	12104
Unique data	5688	11458
Unique data with $I \geq 3.0\sigma(I)$	4573	6068
No. of parameters	364	727
$R^a$	0.060	0.081
$R_w^b$	0.060	0.093
Weighting scheme	$W^{-1} = \sigma^2(F) + 0.000053F^2$	$W^{-1} = \sigma^2(F) + 0.159052F^2$
Largest shift/esd, final cycle	0.03	0.09
Largest peak ( $\text{e}\text{\AA}^{-3}$ )	1.51	1.32

$$^a R = \sum[|F_o| - |F_c|] / \sum|F_o|$$

$$^b R_w = \sum_w^{1/2}[|F_o| - |F_c|] / \sum_w^{1/2}|F_o|$$

tent with the solid-state structure (see below), in which there are clearly two different environments for the methylene protons, namely exo and endo to the ring. The observation of a singlet for these protons can be accounted for in two ways: an accidental equivalence of chemical shifts for the different protons; or the occurrence of a fluxional process which, on the NMR timescale, is fast at room temperature. The former seems unlikely due to the known differences in chemical shifts of exo and endo ring protons in a variety of organic systems, and evidence for a fluxional process comes from variable temperature  $^1\text{H}$  NMR spectroscopy. Thus, upon cooling on acetone- $d_6$  solution of **1**, the low field signal gradually broadens such that at  $-80^\circ\text{C}$  it has gone into the baseline. Unfortunately,

owing to poor solubility, we were unable to reduce the temperature further. We associate the spectral changes with the freezing out of a fluxional process that interconverts endo and exo methylene and phenyl groups.

Construction of a simple molecular model reveals, as expected, that the 14-membered dimetallacyclic ring is highly conformationally flexible and, while a number of fluxional processes might be invoked, interconversion of exo and endo ring positions requires a transition state with a plane of symmetry that includes all ring atoms. Such a state occurs upon interconversion of chair and boat forms of the ring, as shown in Fig. 1.

Iggo and Shaw [11] have previously described the synthesis of somewhat related 10-membered dimetallacyclic  $[(\text{M}(\text{CO})_4(\mu\text{-DPPE}))_2]$  ( $\text{M} = \text{Cr}, \text{Mo}, \text{W}$ ) which

Table 2  
Atomic coordinates ( $\times 10^4$ ) and equivalent isotropic displacement parameters ( $\text{\AA}^2 \times 10^3$ ) for **1** · MeOH

Atom	x	y	z	$U_{\text{eq}}$
Mo(1)	7764(7)	18409(6)	25980(5)	33(1)
P(1)	2001(2)	1622(2)	698(1)	30(1)
P(2)	2670(2)	1815(2)	3319(1)	35(1)
O(1)	-762(10)	4816(7)	2473(7)	101(5)
O(2)	2190(8)	-1152(6)	2632(5)	73(4)
O(3)	-1809(7)	1831(8)	2101(6)	80(4)
O(4)	-1196(8)	2114(8)	4823(5)	86(4)
C(1)	-159(10)	3748(9)	2531(7)	57(5)
C(2)	1706(9)	-87(8)	2612(6)	44(4)
C(3)	-844(8)	1815(7)	2301(6)	46(4)
C(4)	-445(9)	2021(9)	4030(6)	53(4)
C(5)	3305(7)	-51(6)	167(5)	35(3)
C(6)	4045(7)	-233(6)	-918(5)	34(3)
C(7)	4528(8)	483(7)	2855(5)	43(3)
C(8)	5306(7)	358(6)	1785(6)	36(3)
C(10)	718(7)	2060(7)	6(5)	35(3)
C(11)	568(8)	1159(8)	-475(6)	43(4)
C(12)	-465(10)	1556(10)	-963(6)	59(5)
C(13)	-1324(10)	2823(12)	-980(8)	75(6)
C(14)	-1184(11)	3699(11)	-491(10)	87(6)
C(15)	-176(10)	3333(9)	11(8)	65(5)
C(20)	3007(7)	2485(6)	89(5)	32(3)
C(21)	3599(7)	2905(6)	636(6)	36(3)
C(22)	4483(9)	3455(7)	177(6)	47(4)
C(23)	4727(10)	3638(8)	-823(7)	57(5)
C(24)	4103(10)	3272(9)	-1383(6)	58(5)
C(25)	3230(9)	2708(8)	-934(6)	48(4)
C(30)	2361(8)	1562(8)	4660(5)	42(4)
C(31)	2416(11)	2327(9)	5333(6)	63(5)
C(32)	2265(13)	2044(12)	6326(8)	83(7)
C(33)	2081(11)	1008(13)	6633(7)	81(7)
C(34)	2016(14)	273(14)	5972(8)	96(9)
C(35)	2155(12)	543(11)	4979(7)	76(7)
C(40)	2922(8)	3250(7)	3262(5)	40(4)
C(41)	1722(9)	4405(8)	3576(7)	52(4)
C(42)	1831(11)	5524(9)	3541(7)	61(5)
C(43)	3156(12)	5496(9)	3165(7)	63(6)
C(44)	4379(11)	4348(9)	2824(7)	59(5)
C(45)	4288(9)	3199(9)	2870(6)	52(4)
O(5)	5969(11)	5346(10)	4343(8)	119(3)
C(101)	5093(16)	6260(14)	4559(11)	66(4)
C(102)	5448(43)	4353(35)	4905(30)	84(11)

Equivalent isotropic  $U$  defined as one third of the trace of the orthogonalized  $U_{ij}$  tensor.

Table 3

Atomic coordinates ( $\times 10^4$ ) and equivalent isotropic displacement parameters ( $\text{\AA}^2 \times 10^3$ ) for  $2 \cdot 4\text{H}_2\text{O}$ 

Atom	x	y	z	$U_{\text{eq}}$
Mo(1)	48379(7)	17537(7)	16321(6)	49(1)
Mo(2)	89378(7)	7727(7)	2026(7)	57(1)
Mo(3)	76708(9)	49168(7)	3359(9)	72(1)
Mo(4)	69229(7)	25080(6)	1993(6)	42(1)
P(1)	5509(2)	2676(2)	1939(2)	48(2)
P(2)	4801(2)	2082(2)	555(2)	47(2)
P(3)	8110(2)	776(2)	1027(2)	50(2)
P(4)	8092(2)	973(2)	-587(2)	50(2)
P(5)	7371(3)	4318(2)	-583(2)	63(2)
P(6)	8508(2)	4120(2)	647(2)	57(2)
O(1)	6183(8)	1073(7)	1781(7)	98(7)
O(2)	3405(8)	2346(9)	1733(6)	117(8)
O(3)	4638(8)	1327(8)	2924(7)	102(7)
O(4)	4132(9)	555(7)	1270(8)	113(8)
O(5)	8689(9)	-643(8)	26(8)	114(8)
O(6)	9145(9)	2087(8)	655(8)	113(8)
O(7)	10187(9)	537(10)	976(9)	138(9)
O(8)	9969(9)	857(10)	-798(9)	141(10)
O(9)	8563(11)	5798(10)	-430(10)	164(11)
O(10)	6770(9)	4257(8)	1263(9)	120(9)
O(11)	8152(13)	5820(10)	1335(13)	193(14)
O(12)	6426(10)	5746(8)	111(14)	198(16)
O(13)	6362(8)	2448(7)	-1094(8)	97(7)
C(1)	5726(11)	1333(10)	1719(8)	67(8)
C(2)	3913(11)	2170(11)	1677(8)	76(9)
C(3)	4730(9)	1513(9)	2465(9)	67(8)
C(4)	4398(9)	990(9)	1402(9)	69(8)
C(5)	8787(11)	-122(11)	78(9)	76(9)
C(6)	9098(13)	1609(12)	458(12)	106(11)
C(7)	9717(11)	646(13)	718(10)	99(11)
C(8)	9570(11)	800(10)	-445(12)	92(10)
C(9)	8275(14)	5448(11)	-181(12)	101(11)
C(10)	7085(11)	4456(9)	925(11)	75(9)
C(11)	7988(13)	5466(13)	1018(14)	114(13)
C(12)	6909(14)	5452(10)	171(14)	119(13)
C(13)	6563(10)	2467(7)	-637(9)	62(7)
C(14)	6318(7)	2757(7)	1580(7)	46(6)
C(15)	6348(8)	2684(7)	944(7)	42(6)
C(16)	5968(7)	2688(7)	491(7)	41(6)
C(17)	5238(8)	2751(8)	346(8)	58(7)
C(18)	7667(8)	1492(7)	1115(7)	50(6)
C(19)	7357(8)	1750(7)	563(9)	52(7)
C(20)	7189(7)	1624(7)	24(7)	42(6)
C(21)	7218(8)	1121(6)	-366(7)	45(6)
C(22)	7702(8)	3563(7)	-654(6)	46(6)
C(23)	7516(7)	3157(6)	-151(6)	38(4)
C(24)	7635(8)	3119(7)	407(7)	48(4)
C(25)	8123(9)	3390(7)	866(7)	55(6)
C(26)	5086(9)	3374(8)	1837(8)	55(5)
C(27)	5292(10)	3813(9)	1439(9)	73(6)
C(28)	4945(11)	4350(11)	1341(10)	92(7)
C(29)	4387(12)	4448(11)	1670(10)	93(7)
C(30)	4165(13)	4026(11)	2068(11)	103(8)
C(31)	4516(10)	3492(9)	2136(9)	73(6)
C(32)	5804(9)	2722(8)	2688(8)	63(5)
C(33)	6075(10)	2256(10)	2975(9)	75(6)
C(34)	6345(10)	2266(10)	3530(9)	82(6)
C(35)	6303(12)	2806(12)	3843(12)	107(8)
C(36)	6048(12)	3280(11)	3586(11)	95(7)
C(37)	5801(10)	3250(10)	3022(9)	82(6)
C(38)	3943(9)	2247(9)	352(8)	66(5)
C(39)	3507(10)	1748(10)	256(9)	81(6)

Table 3 (continued)

Atom	x	y	z	$U_{eq}$
C(40)	2809(10)	1911(10)	167(9)	77(6)
C(41)	2605(16)	2476(12)	164(12)	121(9)
C(42)	3016(13)	2927(13)	279(11)	109(8)
C(43)	3716(12)	2849(11)	371(10)	94(7)
C(44)	5050(8)	1557(8)	-33(7)	55(5)
C(45)	5328(9)	1022(8)	89(8)	58(5)
C(46)	5523(10)	643(9)	-353(9)	75(6)
C(47)	5445(10)	833(9)	-937(9)	73(6)
C(48)	5184(9)	1353(9)	-1066(9)	69(5)
C(49)	4985(9)	1736(9)	-614(8)	68(5)
C(50)	7482(8)	189(7)	1002(7)	44(4)
C(51)	6811(9)	279(8)	879(7)	57(5)
C(52)	6369(11)	-210(9)	869(9)	75(6)
C(53)	6579(11)	-749(10)	994(9)	82(6)
C(54)	7252(11)	-847(11)	1105(9)	88(7)
C(55)	7697(11)	-382(9)	1124(9)	78(6)
C(56)	8406(11)	674(10)	1784(9)	78(6)
C(57)	7992(16)	621(13)	2235(13)	129(10)
C(58)	8228(19)	567(14)	2824(16)	144(11)
C(59)	8789(23)	508(18)	2938(20)	182(15)
C(60)	9176(27)	508(25)	2549(22)	235(22)
C(61)	9022(21)	709(17)	1926(17)	179(15)
C(62)	8006(8)	350(8)	-1078(7)	54(4)
C(63)	8480(11)	258(10)	-1546(9)	83(6)
C(64)	8466(13)	-237(11)	-1892(11)	97(7)
C(65)	7994(12)	-655(11)	-1832(11)	100(7)
C(66)	7521(14)	-619(13)	-1431(12)	119(9)
C(67)	7541(11)	-102(9)	-1054(10)	81(6)
C(68)	8215(9)	1607(8)	-1096(7)	55(5)
C(69)	8706(10)	2016(9)	-996(9)	74(6)
C(70)	8796(12)	2505(10)	-1376(10)	92(7)
C(71)	8394(12)	2574(11)	-1841(11)	100(7)
C(72)	7913(12)	2171(11)	-1957(11)	93(7)
C(73)	7812(10)	1680(9)	-1570(9)	76(6)
C(74)	6472(9)	4170(8)	-735(8)	64(5)
C(75)	6025(12)	4263(10)	-335(11)	95(7)
C(76)	5339(12)	4122(10)	-447(11)	92(7)
C(77)	5196(13)	3933(10)	-936(10)	93(7)
C(78)	5596(12)	3832(11)	-1368(11)	99(7)
C(79)	6298(11)	3988(9)	-1275(9)	80(6)
C(80)	7661(10)	4695(9)	-1273(8)	65(5)
C(81)	7381(12)	5243(11)	-1382(10)	96(7)
C(82)	7657(13)	5533(13)	-1939(12)	113(9)
C(83)	8100(14)	5317(12)	-2244(13)	114(8)
C(84)	8325(13)	4762(11)	-2118(11)	103(8)
C(85)	8107(11)	4449(11)	-1612(10)	93(7)
C(86)	9150(8)	3929(7)	133(7)	46(4)
C(87)	9398(14)	4336(14)	-223(12)	122(9)
C(88)	9868(15)	4206(14)	-648(14)	133(10)
C(89)	10182(12)	3656(11)	-636(11)	94(7)
C(90)	9961(12)	3248(12)	-311(11)	103(7)
C(91)	9467(13)	3379(12)	123(12)	115(8)
C(92)	8955(11)	4307(9)	1315(9)	78(6)
C(93)	8583(12)	4425(10)	1832(10)	89(7)
C(94)	8882(17)	4553(14)	2383(15)	141(11)
C(95)	9518(17)	4579(14)	2368(16)	144(11)
C(96)	9937(20)	4466(15)	1902(15)	157(12)
C(97)	9645(12)	4305(10)	1350(11)	100(7)
O(100)	878(9)	2008(9)	506(8)	128(6)
O(101)	7231(12)	7942(12)	2470(11)	181(9)
O(102)	1238(15)	2200(14)	2343(13)	213(11)
O(103)	6522(17)	7213(16)	1316(14)	247(13)

Equivalent isotropic  $U$  defined as one third of the trace of the orthogonalized  $U_{ij}$  tensor.

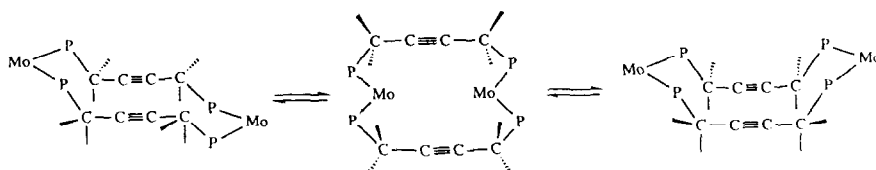


Fig. 1. Equivalencing of endo and exo methylene protons in **1** via a chair–boat interconversion.

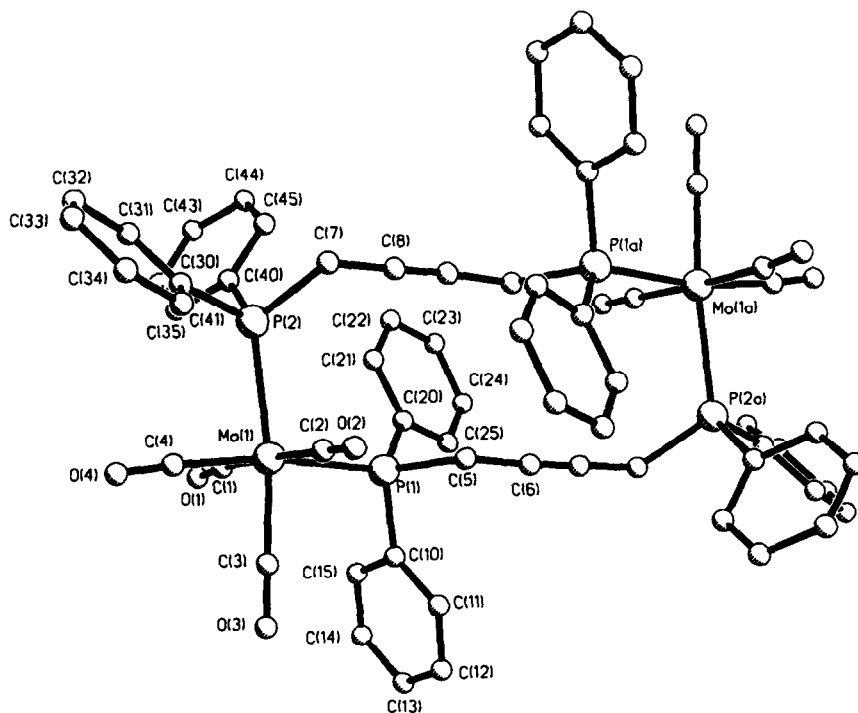


Fig. 2. Molecular structure of  $[(\text{Mo}(\text{CO})_4(\mu\text{-DPPBu}))_2]$  (**1**).

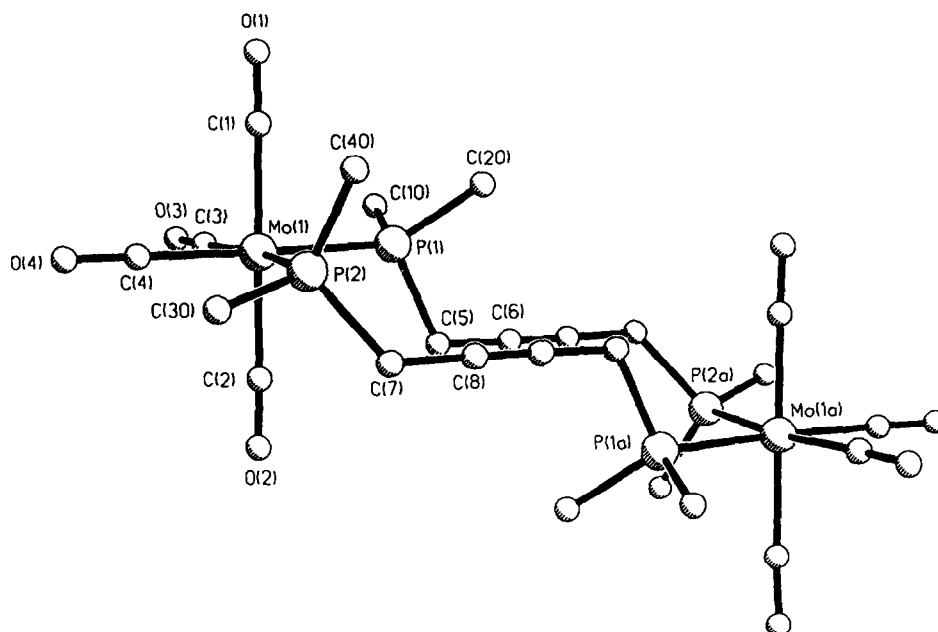


Fig. 3. Molecular structure of  $[(\text{Mo}(\text{CO})_4(\mu\text{-DPPBu}))_2]$  (**1**) with phenyl group omitted for clarity.

Table 4  
Selected bond length (Å) and angles (°) for  $[(\text{Mo}(\text{CO})_2(\mu\text{-DPPBu}))_2](1)$

Mo(1)–P(1)	2.551(2)	Mo(1)–P(2)	2.572(3)
Mo(1)–C(1)	2.029(9)	Mo(1)–C(2)	2.042(9)
Mo(1)–C(3)	1.967(11)	Mo(1)–C(4)	1.998(7)
C(5)–C(6)	1.460(9)	C(7)–C(8)	1.455(10)
C(6)–C(8A)	1.181(10)		
P(1)–Mo(1)–P(2)	102.8(1)	C(1)–Mo(1)–C(2)	177.7(4)
C(3)–Mo(1)–C(4)	83.4(4)	P(1)–Mo(1)–C(4)	170.9(3)
P(2)–Mo(1)–C(3)	169.4(2)	Mo(1)–P(1)–C(5)	112.8(2)
Mo(1)–P(2)–C(7)	118.5(3)	P(1)–C(5)–C(6)	115.3(5)
P(2)–C(7)–C(8)	116.7(5)	C(5)–C(6)–C(8A)	176.3(11)
C(7)–C(8)–C(6A)	178.8(7)		

are also fluxional at room temperature. For example, at this temperature homobimetallic complexes display a singlet in the  $^{31}\text{P}$  NMR spectrum which upon cooling to  $-90^\circ\text{C}$  (for chromium) collapses into AB doublets, the phosphorus–phosphorus coupling constant of 28 Hz being indicative of a relative *cis*-orientation of inequivalent phosphorus centres. The nature of this fluxional process was not fully elucidated.

In order to fully elucidate the structure of **1** in the solid-state, a crystallographic study was carried out on a methanol solvate, the results of which are summarised in Figs. 2 and 3 and Table 4. The molecule adopts a chair configuration, with one half being unique and related to the second by the inversion centre. The two phosphorus centres subtend a “bite-angle” of  $102.8^\circ$  at molybdenum, which is significantly greater than those found in the related rigid-backbone diphosphine complex  $[(\text{Mo}(\text{CO})_4(\mu\text{-DPPA}))_2]$  ( $93.1(1)$  and  $96.5(1)^\circ$  [1]),

indicating that there is less ring strain in the former. The chair geometry is defined by the *anti*-configuration of phosphorus centres on each diphosphine. The central carbon atoms lie approximately in a plane, the greatest deviation being  $0.014 \text{ \AA}$  by C(8), with planes containing the metal and phosphorus atoms lying approximately  $1.6 \text{ \AA}$  above and below a the latter. The central core of the molecule is unperturbed upon metal coordination, with distinct single [C(5)–C(6)  $1.460(9)$ ; C(7)–C(8)  $1.455(10) \text{ \AA}$ ] and triple [C(6)–C(8A)  $1.181(10) \text{ \AA}$ ] bonds, while the linearity of the central  $\text{C}_4$  unit is maintained [C(5)–C(6)–C(8A)  $176.3(11)$ ; C(7)–C(8)–C(6A)  $178.8(7)^\circ$ ]. Bond angles at both phosphorus [Mo(1)–P(1)–C(5)  $112.8(2)$ ; Mo(1)–P(2)–C(7)  $118.7(3)^\circ$ ] and methylene carbons [P(1)–C(5)–C(6)  $115.3(5)$ ; P(2)–C(7)–C(8)  $116.7(5)^\circ$ ] do, however, differ from the idealised tetrahedral value, which may indicate a degree of ring strain. The preferences for the

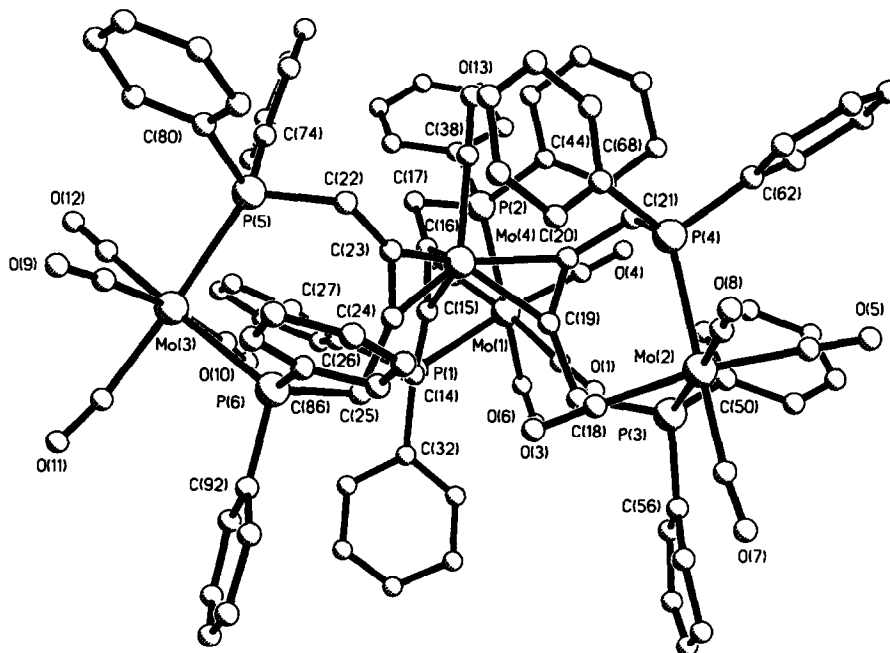


Fig. 4. Molecular structure of  $[(\text{Mo}(\text{CO})_4(\eta^2\text{-DPPBu}))_3[\text{Mo}(\text{CO})]](2)$ .



chair over the boat conformation may result from adverse steric interactions between endo phenyl rings in the latter. A packing diagram revealed no short intermolecular interactions or noticeable packing of the chairs. In view of the large ring size, energy differences between chair and boat conformations are not expected to be large and thus interconversion may be facile.

While a number of dimetallacyclic complexes containing two molybdenum tetracarbonyl units have previously been crystallographically characterised [1,2,12,13], larger rings (16 atoms or greater) contain a *trans* rather than *cis* relative orientation of the phosphines [12,13]. For example, Ueng and Hwang have shown that this is the case for both 16- and 18-membered rings  $[\{\text{Mo}(\text{CO})_4(\mu\text{-Ph}_2\text{P}(\text{CH}_2)_n\text{PPh}_2)_2\}]$  ( $n = 5$  [12],  $n = 6$  [13]). In contrast, the saturated 4-atom backbone diphosphine ( $n = 4$ ) does not form a dimetallacycle of this type, but rather the chelate complex  $[\text{Mo}(\text{CO})_4(\eta^2\text{-Ph}_2\text{P}(\text{CH}_2)_4\text{PPh}_2)]$  is isolated, which has also been crystallographically characterised [14].

Characterisation of  $[\{\text{Mo}(\text{CO})_4(\eta^2\text{-DPPBu})\}_3\{\text{Mo}(\text{CO})\}]$  (**2**) on the basis of spectroscopic data proved more problematical. The IR spectrum, while containing absorptions indicative of a *cis*-disubstituted molybdenum tetracarbonyl unit, also showed a weak, but persistent, absorption at  $2066\text{ cm}^{-1}$ , indicative of a further molybdenum carbonyl-containing species. Both  $^{31}\text{P}$  and  $^1\text{H}$  NMR spectra suggested that ends of the diphosphine differed, since two phosphorus and methylene environ-

ments were observed respectively. In the former, the phosphorus–phosphorus coupling constant of 27.7 Hz is again indicative of a *cis*-arrangement of phosphorus atoms.

Crystallisation of **2** upon slow evaporation of a 1,2-dichloropropane–light petroleum mixture in air afforded small yellow plates analysing as  $2 \cdot 4\text{H}_2\text{O}$ , which were suitable for X-ray crystallography (the results of which are summarised in Figs. 4 and 5 and Table 5). Owing to the large cell volume and small crystal size, estimated standard deviations are quite high, however, gross structural features, notably the conformation of the central core of the molecule, are worthy of discussion. The molecule consists of three molybdenum tetracarbonyl–DPPBu units, linked to a further molybdenum carbonyl fragment via coordination of the carbon–carbon triple bonds of the diphosphine. In the latter respect, it is closely analogous to  $[\text{Mo}(\text{CO})(\eta^2\text{-PhC}_2\text{Ph})_3]$  [15], the structure of which has recently been published [16]. Thus, in **2** each diphosphine a molybdenum tetracarbonyl moiety, the bite-angle ranging from  $91.0(2)$  to  $94.6(2)^\circ$ , being similar to that of  $91.65(4)^\circ$  found in the related saturated complex  $[\text{Mo}(\text{CO})_4(\eta^2\text{-Ph}_2\text{P}(\text{CH}_2)_4\text{PPh}_2)]$  [14]. The backbones of the diphosphine ligands are significantly folded, roughly along an axis including that of the methylene carbons and the phosphorus centre opposite, such that one phosphorus and the four carbon atoms of the backbone lie approximately in a plane. The triple bond of each diphosphine is further coordinated to

Table 5  
Selected bond lengths (Å) and angles (°) for  $[\{\text{Mo}(\text{CO})_2(\eta^2\text{-DPPBu})\}_3\{\text{Mo}(\text{CO})\}]$  (**2**)

Mo(1)–P(1)	2.554(5)	Mo(1)–P(2)	2.556(5)
Mo(2)–P(3)	2.552(5)	Mo(2)–P(4)	2.510(5)
Mo(3)–P(5)	2.549(6)	Mo(3)–P(6)	2.548(5)
Mo(1)–C(1)	2.033(22)	Mo(1)–C(2)	2.089(23)
Mo(1)–C(3)	1.982(20)	Mo(1)–C(4)	1.985(20)
Mo(2)–C(5)	2.035(24)	Mo(2)–C(6)	1.976(26)
Mo(2)–C(7)	1.976(23)	Mo(2)–C(8)	1.957(25)
Mo(3)–C(9)	2.070(26)	Mo(3)–C(10)	2.066(23)
Mo(3)–C(11)	2.073(30)	Mo(3)–C(12)	1.981(26)
Mo(4)–C(13)	2.035(21)	Mo(4)–C(15)	2.096(16)
Mo(4)–C(16)	2.083(15)	Mo(4)–C(19)	2.071(16)
Mo(4)–C(20)	2.079(16)	Mo(4)–C(23)	2.043(15)
Mo(4)–C(24)	2.033(16)	C(15)–C(16)	1.278(22)
C(19)–C(20)	1.300(25)	C(23)–C(24)	1.293(21)
P(1)–Mo(1)–P(2)	92.5(1)	P(3)–Mo(2)–P(4)	94.6(2)
P(5)–Mo(3)–P(6)	91.0(2)	C(1)–Mo(1)–C(2)	171.6(7)
C(3)–Mo(1)–C(4)	88.2(8)	P(1)–Mo(1)–C(4)	174.3(6)
P(2)–Mo(1)–C(3)	171.9(6)	C(5)–Mo(2)–C(6)	170.9(9)
C(7)–Mo(2)–C(8)	86.0(10)	P(3)–Mo(2)–C(8)	177.9(7)
P(4)–Mo(2)–C(7)	170.1(7)	C(9)–Mo(3)–C(10)	173.6(9)
C(11)–Mo(3)–C(12)	91.3(11)	P(5)–Mo(3)–C(11)	173.1(8)
P(6)–Mo(3)–C(12)	170.1(8)	C(16)–Mo(4)–C(20)	119.0(6)
C(20)–Mo(4)–C(23)	116.2(6)	C(16)–Mo(4)–C(23)	122.4(6)
C(14)–C(15)–C(16)	140.3(15)	C(15)–C(16)–C(17)	138.9(15)
C(18)–C(19)–C(20)	143.6(15)	C(19)–C(20)–C(21)	138.0(15)
C(22)–C(23)–C(24)	137.7(14)	C(23)–C(24)–C(25)	138.3(15)

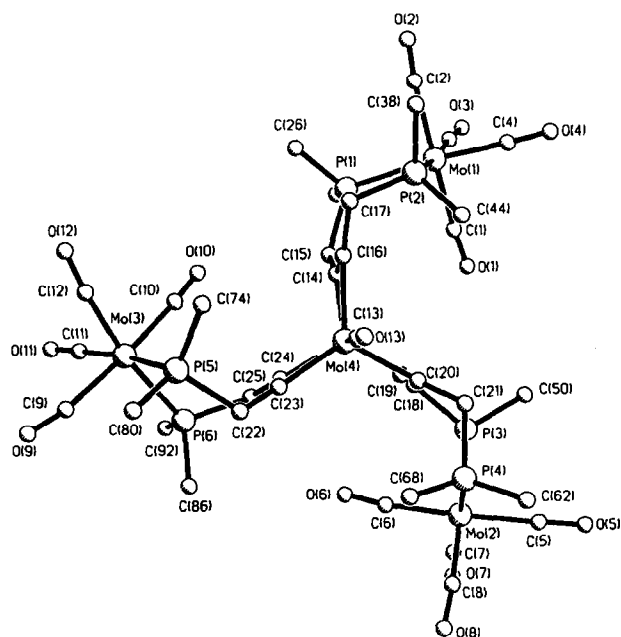


Fig. 5. Molecular structure of  $[(\text{Mo}(\text{CO})_4(\eta^2\text{-DPPBu}))_3(\text{Mo}(\text{CO}))]$  (**2**) with phenyl groups omitted for clarity.

the central molybdenum centre in such a way that the carbon–carbon vectors lie approximately parallel to the unique molybdenum carbonyl vector. Coordination of the triple bond results in a pronounced lengthening from the value of 1.181(10) Å in **1** to between 1.278(22) and 1.300(25) Å, which is also associated with a pronounced decrease in the linearity of the  $\text{C}_4$  backbone. Thus,  $\text{CH}-\text{C}\equiv\text{C}$  angles now range between 137.7(14) and 143.6(15)°, the average being 139.5°. While the increase in length of the triple bond is similar to that seen in  $[\text{Mo}(\text{CO})(\eta^2\text{-PhC}_2\text{Ph})_3]$  [16], the decrease in the bond angles at the acetylinic carbons is more pronounced, ranging from 147.0(5) to 150.8(8)° in the latter. This approximate 10° difference is likely to be a result of constraining the coordinated alkyne into a metallacycle. The unique carbonyl is not significantly different from those of the molybdenum tetracarbonyl units, with the latter showing the familiar lengthening of *cis* and shortening of *trans* metal–carbon distances.

Overall, viewed down the O(13)–C(13)–Mo(4) axis (Fig. 5), **2** has approximate three-fold symmetry. Szymanska-Buzar and Glowiak [16] have previously described the central core of  $[\text{Mo}(\text{CO})(\eta^2\text{-PhC}_2\text{Ph})_3]$  as a capped trigonal prism with the carbonyl acting as the capping group, and a similar description of **2** is also apt. Indeed, it is the presence of the unique carbonyl that renders phosphorus and methylene centres inequivalent. Generally, alkyne rotation at a metal centre is considered to be facile and the occurrence of such a process in **2** would render the phosphorus centre equivalent. The sharp lines in the  $^{31}\text{P}$  NMR spectrum suggest (at least at

room temperature) the absence of such a process. In order to obey the 18-electron rule, each alkyne must formally donate  $3\frac{1}{2}$  electrons to the central molybdenum atom, and this is consistent with King's [17] rationalisation of the bonding in  $[\text{W}(\text{CO})(\eta^2\text{-PhC}_2\text{Ph})_3]$ .

The nature of the minor reaction component **3** remains unknown. The only reliable data is the  $^{31}\text{P}$  NMR spectrum which shows doublets at 28.8 and 23.5 ppm, the phosphorus–phosphorus coupling constant of 23.5 Hz being indicative of a *cis*-disubstituted complex. A likely candidate might appear to be  $[\text{Mo}(\text{CO})_4(\eta^2\text{-DP-PBu})]$ , however, it is not immediately apparent how the inequivalence of phosphorus centres arises. The latter represents coordination mode B invoked in the Introduction. Such a chelate complex is expected to be highly strained, indeed construction of a simple model requires a degree of bending at the acetylinic carbons. In light of the formation of **2**, which displays both bonding modes B and C, it is interesting to consider whether the former can exist without the latter, which in turn lends some insight into the mode of formation of **2**. Certainly, the considerable ring strain anticipated for a simple chelate complex will be significantly relieved as an olefinic character develops upon coordination of the alkyne. It seems more likely, however, that competitive formation of **1** and **2** results from initial coordination of phosphorus or the carbon–carbon triple bond respectively to the coordinatively labile *cis*- $[\text{Mo}(\text{CO})_4(\text{piperidine})_2]$ . It is difficult to imagine that this initial product of phosphorus coordination, namely  $[\text{Mo}(\text{CO})_4(\text{piperidine})(\eta^1\text{-DP-PBu})]$  will undergo an intramolecular displacement to afford the strained chelate complex more rapidly than an intermolecular reaction with a further equivalent of diphosphine or the molybdenum complex, both of which would result in formation of **1**.

## References

- [1] G. Hogarth and T. Norman, *Polyhedron*, in press.
- [2] G. Hogarth and T. Norman, *J. Chem. Soc., Dalton Trans.*, in press.
- [3] G. Hogarth and T. Norman, *Inorg. Chim. Acta*, in press.
- [4] G. Maier, S. Pfriend, U. Schäfer, K.-D. Malsch and R. Matusch, *Chem. Ber.*, **114** (1981) 3965.
- [5] M. Arthurs S.M. Nelson and B.J. Walker, *Tetrahedron Lett.*, **13** (1978) 1153; D.G. Gillespie and B.J. Walker, *J. Chem. Soc., Perkin Trans. 1*, (1983) 1689.
- [6] R.B. King and A. Efraty, *Inorg. Chim. Acta.*, **4** (1970) 123.
- [7] O. Orama, *J. Organomet. Chem.*, **314** (1986) 273 and references cited therein.
- [8] T.M. Nickel, S.Y.W. Yau and M.J. Went. *J. Chem. Soc., Chem. Commun.*, (1989) 775.
- [9] D.J. Darensbourg and R.L. Kump, *Inorg. Chem.*, **17** (1978) 2680.
- [10] G.M. Sheldrick, *SHELXTL PLUS, Program package for structure solution and refinement*. Vers. 4.2. Siemens Analytical Instruments Inc., Madison, WI, 1990.

- [11] J.A. Iggo and B.L. Shaw, *J. Chem. Soc., Dalton Trans.*, (1985) 1009.
- [12] C.-H. Ueng and J.-L. Hwang, *Acta Crystallogr.*, 50 (1994) 1866.
- [13] C.-H. Ueng and G.-Y. Hwang, *J. Chem. Soc., Dalton Trans.*, (1991) 1643.
- [14] C.-H. Ueng and G.-Y. Hwang, *Inorg. Chim. Acta*, 218 (1994) 9.
- [15] W. Strohmeter and D. Hobe, *Z. Naturforsch.*, 19B (1964) 959.
- [16] T. Szymanska-Buzar and T. Glowiak, *J. Organomet. Chem.*, 467 (1994) 223.
- [17] R.B. King, *Inorg. Chem.*, 7 (1968) 1044.